TABLE OF CONTENTS

		page	
	SUMMARY	1	1/A5
I.	INTRODUCTION	3	1/A7
	A. Background	3	1/A7
	B. Statement of Problem	4	1/A8
	C. Salient Results	6	1/A10
II.	THEORY OF COUPLED WAVE MODEL	9	1/A13
	A. Evolution of Model	9	1/A13
	B. Formal Solution	15	1/B5
	C. Two-Turn Coil	20	1/B10
III.	TESTS ON A TWO-TURN COIL	23	1/B13
	A. Frequency Response	23	1/B13
	B. Decay of Initial Current	26	1/C3
	C. An Experimental Test	35	1/C12
IV.	CONCLUSION AND RECOMMENDATIONS	44	1/D7
	APPENDIX	47	1/D10
	REFERENCES	49	1/D12

830-H-14

NASA 1.26:3332

NASA Contractor Report 3332

COMPLETED
ORIGINAL

Coupled Wave Model for Large Magnet Coils

G. J. Gabriel

GRANT NSG-3182
SEPTEMBER 1980

NASA

54

NASA Contractor Report 3332

Coupled Wave Model for Large Magnet Coils

G. J. Gabriel
University of Notre Dame
Notre Dame, Indiana

Prepared for
Lewis Research Center
under Grant NSG-3182

National Aeronautics
and Space Administration

**Scientific and Technical
Information Branch**

1980

BLANK PAGE

BLANK PAGE

SUMMARY

An important problem in the design of large superconducting magnets is that of protecting the coil against high voltage breakdown due to electromagnetic transients which might be initiated by any of a number of causes such as faults, quenches, or switching. An understanding of such transients as the key to coil protection provided the motivation for this investigation and its objective of evolving a suitable analytical model that would help in the design of protective measures. Inadequacy of existing circuit theoretic models to account for effects observed in an earlier work necessitated a detailed field theoretic analysis which has resulted in the coupled wave model (CWM) based on the theory of multiconductor transmission line theory. Significantly, this model shows that, unlike the predictions of circuit theory, the temporal response of a coil at its terminals unfolds in discrete steps having durations equal to the travel time of a wave front around a single turn of winding. It is during one or more of these steps that high voltages are likely to occur. Thus the size of a coil becomes an important consideration in design.

Successful results of detailed computational and experimental analysis of a two turn coil indicate that the model is of sufficient merit to warrant further refinement, if need be, and to justify detailed analysis of the general case of a multiconductor coil. Notably, both the high frequency and low frequency behavior are

incorporated in the model where, it is found that the turn-to-turn coupling coefficients play a significant role. While these coefficients are related to such factors as wire size, shape, and packing factor, design specifications cannot be firmly established at this stage of the development.

I. INTRODUCTION

A. Background

Superconductivity is finding an important application in large, energy efficient d.c. magnets such as those intended for use in magneto-hydrodynamic energy conversion, thermonuclear fusion, and pulsed high power generation. In the current state of the art, such magnets are typically in the form of solenoid or saddle coils of wire composed of superconducting metal imbedded in copper substrate and cryogenically cooled to liquid Helium temperature. Because of their large scale in every respect--current magnitude, energy, physical size--superconducting magnets, as envisaged for the above mentioned applications, pose new problems which heretofore had not been encountered in smaller conventional coils.

Protection of the coil against possible damage, especially that due to high voltage breakdown within the coil, is one such problem which is of major concern to superconducting magnet programs. To guard against damage due to excessive ohmic heating resulting from a sudden quench, typically the coil is switched from the power supply to a set of damping resistors intended to limit the terminal voltage during the current decay, as well as to dissipate the stored magnetic energy. Despite this conventional method or protection, evidence of interlayer voltage breakdown has been observed at NASA-Lewis Research Center upon disassembling a damaged coil [1]. That the voltages anywhere within the coil should not exceed the prescribed terminal voltage, however, is a conclusion based on the circuit theory of lumped inductors and, as such,

ignores the spatial distribution of voltages and currents. Properly, the problem falls in the realm of electrodynamic field theory.

In support of the field theoretic viewpoint, evidence of multiple reflection of waves as well as a multiplicity of resonances due to standing waves on a prototype coil was reported in an earlier work [2]. It was also proposed, then, that multiply reflected wave fronts could provide a mechanism for voltage buildup at appropriate points within the coil. In view of these earlier findings, the need for a more realistic analytical model for predicting the coil behavior became apparent.

The research reported herein was undertaken as a first step toward a better understanding of the electrodynamics of coils which hold the key to the objective of evolving a suitable analytical model that would help in the design of protective methods. To this end, the coupled wave model resulting from this investigation, as discussed in Sec. II, represents a significant refinement over earlier models. It is, however, one step in what is seen to be a continuing evolutionary process.

B. Statement of the Problem

Analytical modeling of the transient behavior of large coils is not new but has a long history in the power industry in connection with large transformers. A search of the literature, however, reveals that existing models are hypothetical, founded exclusively on the principles of circuit theory [3]-[5]. Typically, the coil is divided into an arbitrary number of meshes composed of inductors and capacitors. Moreover, most of the data appear to be restricted to a time scale measured in tens of microseconds which is too coarse for the events

we have observed. The significance of this point in the context of large coils having diameters of, say, one ft or more is appreciated when one considers that an electromagnetic disturbance travels 30 cm (1 ft) in one nanosecond.

A purely network theoretic approach suffers from several disadvantages as follows [6]:

1. There is no principle by which one determines beforehand the number of meshes into which a coil must be subdivided;
2. There is no principle by which one determines the necessity of a particular topography of interconnections among the assumed circuit elements;
3. The nodes and branches of the assumed network model cannot be uniquely identified with actual spatial locations on the physical coil; and
4. Geometric factors pertaining to the coil are not readily manifested in the assumed circuit elements.

Consequently, the thrust of our effort was shifted to a search for a model founded on field theory, even if approximate. A detailed field theoretic solution of the problem, though necessary and desirable in the long run, is replete with difficulties owing to the unorthodox reference frames that even the simplest coil geometry requires. Nevertheless, evidence from a number of experiments on a variety of helical coils, leads to the conclusion that electromagnetic waves propagate along the coil wire itself, and that to a fair degree of approximation they behave as transverse electromagnetic (TEM) waves. Moreover, the waves on one turn of the coil are coupled to those on the others.

On the other hand, analysis of the field equations in a helical coordinate system appropriate to solenoids has shown that, strictly speaking, the electromagnetic field is not separable into the form demanded by the conditions for the existence of TEM waves. A perturbed version of TEM waves, however, is theoretically possible, and these would exhibit certain periodicities owing to the inherent periodicity of helical coordinates. Based on these considerations, the proposed coupled wave model was evolved as a foundation which is amenable to further refinement if need be. This model, together with corroborative computational tests on a two-turn coil, is discussed in the next sections, which are then followed by our conclusions and recommendations.

C. Salient Results

The coupled wave model (CWM) has many interesting features as an analytical model for coils in general. However, it is appropriate at this point to present the three most significant findings as pertaining to the objective of this investigation:

1. All temporal events on the coil, such as decay of initial current through a resistor, evolve in discrete steps having a characteristic duration τ, which is the travel time of a wave front around a single turn. In agreement with observations in time domain reflectometery (TDR) experiments, the theoretical calculations show that over long time scales these steps are smoothed so that response curves approach those expected from circuit theory. This phenomenon is interpreted as being a manifestation of coupled multiple reflections due to proximity and periodicity inherent in the physical structure of any coil.

2. The discrete nature of the coil response is a very significant finding, because high voltages are likely to occur during one of these discrete steps. Thus, if the probability of dielectric breakdown increases with the duration of a high voltage pulse, a large coil is more likely to experience breakdown than a smaller one. Theoretical confirmation is provided by analysis of the decay of initial current in a two-turn coil connected to a resistor. With appropriate combination of parameters, the terminal voltage is found to exceed that predicted by circuit theory by a factor of 1.125. Although this excess of 12.5 percent might not be sufficient to cause breakdown, it serves to illustrate the point that high voltages can occur, given the right conditions.

3 In the earlier work [2] on a prototype four-layer coil, the multiplicity of periodically spaced resonances (at frequencies upward of 600 kHz) was roughly explained in terms of standing waves on a single straight transmission line. This, however, did not account for the low frequency resonance (of the order of 15 kHz) which bears no discernible relation to wire length as expected of standing waves. Existence of this resonance has been known for many decades and it has generally been interpreted in a circuit theoretic context as being a consequence of distributed shunt capacitance. Such circuit models, on the other hand, do not fully describe the high frequency (or short time) behavior of the coil. The coupled wave model bridges the gap. The low frequency resonance, in the sense of a minimum in the terminal admittance, is found to be a direct manifestation of coupling between turns. At frequencies which are small compared to $1/\tau$, the terminal

admittance calculated from the CWM approaches that of a parallel combination of a lumped inductor and capacitor. Although much attention has been given to the low frequency resonance in the literature on transformers, it does not appear to be a serious contender as a cause for high voltage breakdown, as shown in the sequel. It is, however, still important to the extent that it provides one more datum in support of the wave model, and may also prove useful in experimental estimation of coil parameters.

II. THEORY OF COUPLED WAVE MODEL

A. Evolution of the Model

Consider M straight wires, each having a length 2L, arranged in a uniform parallel array lying on a plane as shown in Fig. 1. Such an array is known to support dynamic electromagnetic fields in the TEM mode. The geometry of the array is such that it permits exact solution of Maxwell's equations whereby the electric and magnetic fields, $\underline{E}$ and $\underline{H}$, are separated into the product of functions, i.e.

$$\underline{E}(x,y,\zeta,t) = v'(\zeta,t)\ \underline{e}(x,y) \tag{1}$$

$$\underline{H}(x,y,\zeta,t) = i'(\zeta,t)\ \underline{h}(x,y) \quad . \tag{2}$$

The amplitude functions v' and i' satisfy the one dimensional wave equation in the ζt manifold, and, with appropriate geometric normalization, they can be interpreted as voltage and current insofar as their product yields the total power. The vector functions $\underline{e}$ and $\underline{h}$, on the other hand, are strictly dependent on the cross sectional geometry of the array, since they are derived from a scalar potential which satisfies the two dimensional Laplace quation subject to the boundary constraint imposed by the conductors.

As a consequence of some properties of the Laplace equation, it is possible to associate with each conductor in the array, say the m^{th} one, a "voltage" $v_m(\zeta,t)$ and a current $i_m(\zeta,t)$. Each of these voltages and currents is porportional, respectively, the the field amplitude functions v' and i', while the geometry of the array is manifested in coupling coefficients γ_{mn} relating the m^{th} voltage to the n^{th} current, vice versa.

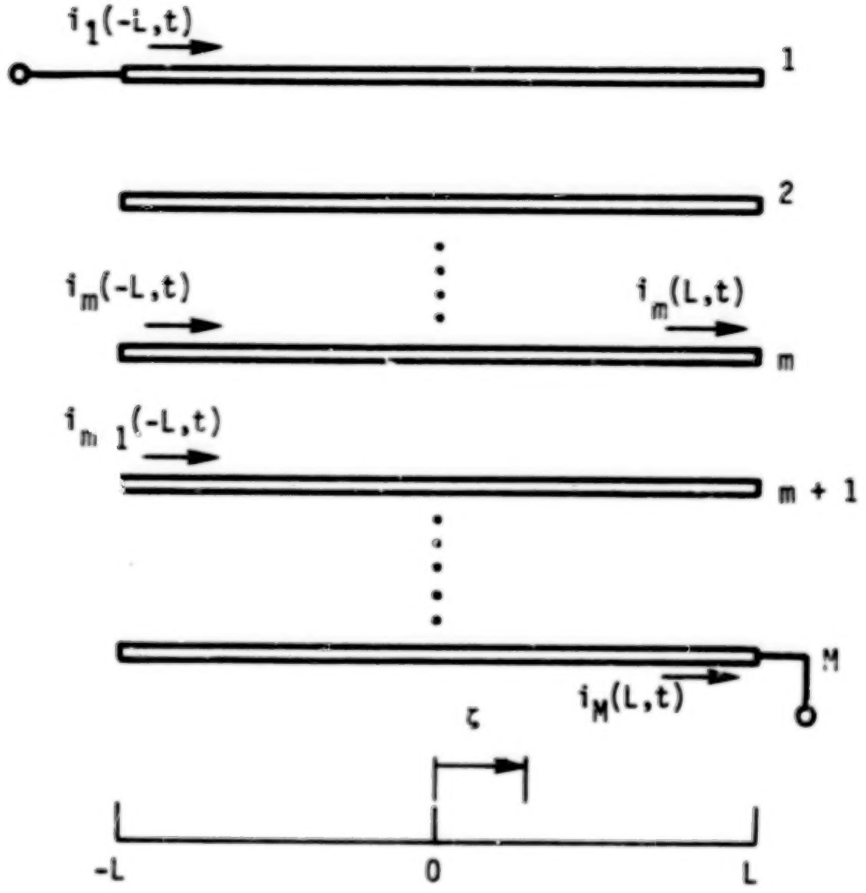

Fig. 1: Straight wire array.

It is most convenient to employ the formalism of matrices and introduce the column vectors

$$\underline{v}(\zeta,t) = \begin{bmatrix} v_1(\zeta,t) \\ \vdots \\ v_M(\zeta,t) \end{bmatrix}, \qquad \underline{i}(\zeta,t) = \begin{bmatrix} i_1(\zeta,t) \\ \vdots \\ i_M(\zeta,t) \end{bmatrix}$$

and the coupling coefficients matrices

$$L = \mu \bar{\gamma}^{-1} \quad , \quad \bar{C} = \varepsilon \bar{\gamma}$$

where ε and μ are the permitivity and permeability of the medium surrounding the wires. Throughout this report matrices are denoted by a bar over the symbols, unless otherwise stated.

With these definitions, the electromagnetic behavior of the array is governed by the system of equations, in matrix form,

$$\frac{\partial}{\partial \zeta} \underline{v}(\zeta,t) = -\bar{L} \frac{\partial}{\partial t} \underline{i}(\zeta,t) \tag{3}$$

$$\frac{\partial}{\partial \zeta} \underline{i}(\zeta,t) = -\bar{C} \frac{\partial}{\partial t} \underline{v}(\zeta,t) \tag{4}$$

These equations are well known as the basis of the theory of coupled TEM transmission lines. For convenience of reference, we call $\bar{L}$ the inductive coupling matrix and $\bar{C}$ the capacitive coupling matrix. They must always satisfy the condition

$$\underline{L}\,\underline{C} = \frac{1}{c^2}\,\underline{I} \tag{5}$$

where c is the speed of wave propagation and $\underline{I}$ is the identity matrix. Consequently, when Equations (3) and (4) are diagonalized, the result is the one dimensional wave equation satisfied by each component of $\underline{v}$ and $\underline{i}$,

$$\frac{\partial^2}{\partial z^2}\begin{bmatrix}\underline{v}\\ \underline{i}\end{bmatrix} - \frac{1}{c^2}\,\frac{\partial^2}{\partial t^2}\begin{bmatrix}\underline{v}\\ \underline{i}\end{bmatrix} = \begin{bmatrix}\underline{0}\\ \underline{0}\end{bmatrix} . \tag{6}$$

In other words, all component voltages and currents travel in unison.

To apply the theory of coupled lines to a coil, let us bend the plane in which the wires lie into a cylindrical surface, joining the right end of the m^{th} wire to the left end of the $(m+1)^{th}$ wire. The result is a single layer solenoidal coil whose terminals correspond to the left end of the first wire and right end of the M^{th} one, as illustrated in Fig. 2.

With each turn of the solenoid now viewed as one line in the M-conductor system, the geometry of the solenoid amounts to imposition of the periodic boundary constraints

$$i_{m+1}(-L,t) - i_m(L,t) = 0, \quad 1 \le m \le M-1 \tag{7}$$

$$i_1(-L,t) = i_M(L,t) = i_t(t)$$

$$v_{m+1}(-L,t) - v_m(L,t) = 0, \quad 1 \le m \le M-1 \tag{8}$$

$$v_1(-L,t) - v_M(L,t) = v_t(t)$$

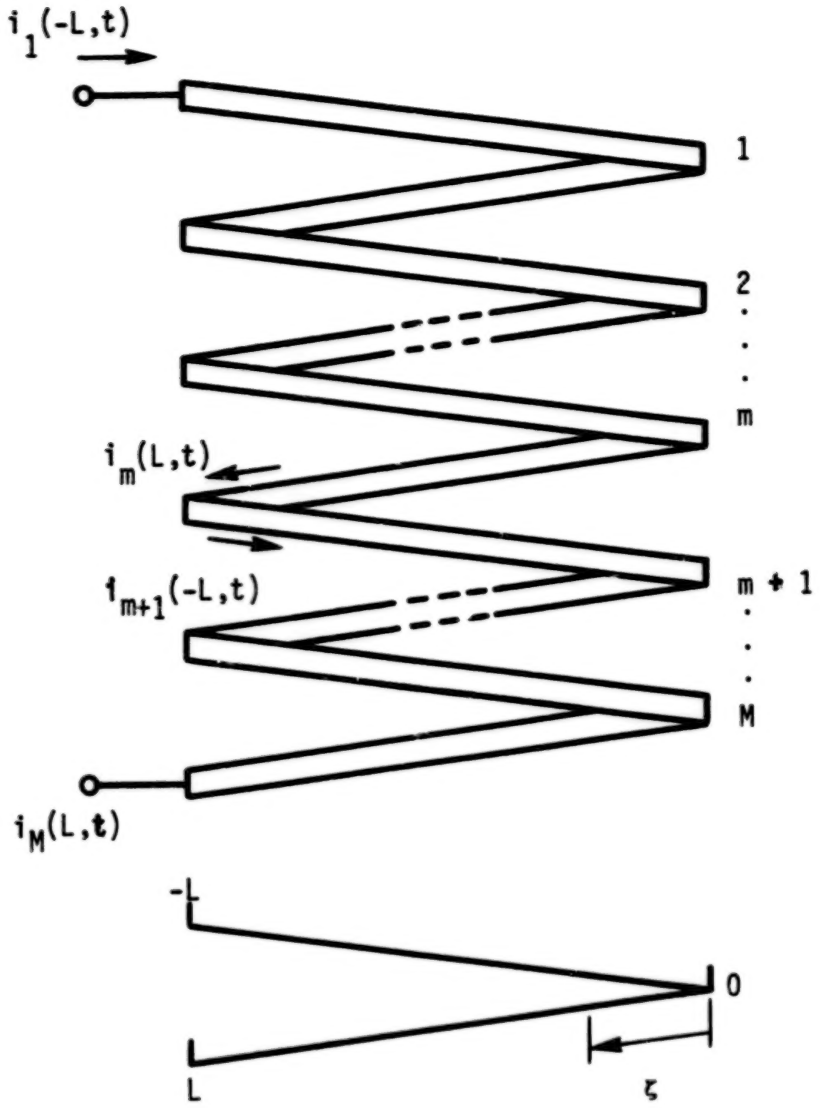

Fig. 2: Helical coil geometry.

where v_t and i_t are the terminal voltage and current. These may be readily put in matrix form by introducing the interconnection matrix $\bar{T}$ whose elements in the case of a solenoid are

$$T_{mn} = \delta_{n,m+1} \qquad 1 \leq m \leq M-1$$
$$T_{Mn} = \delta_{n,1} \tag{9}$$

where the Kronecker delta has the usual meaning. The boundary constraints then take the compact form

$$\bar{T}\,\underline{v}(-L,t) - \underline{v}(L,t) = v_t \underline{a}_M \quad , \tag{10}$$

$$\bar{T}\,\underline{i}(-L,t) - \underline{i}(L,t) = \underline{0} \tag{11}$$

where $\underline{a}_M$ is the normal column vector having zeros in every row except M, and 1 in row M.

It should be noted that every interconnection, including taps, corresponds to a matrix $\bar{T}$, whose columns and rows contain only one non-zero element, which is usually 1. Further, the matrix is always orthogonal having eigenvalues which are the complex roots of 1 on the unit circle in the complex plane. These eigenvalues are significant since they are directly related to the resonances of the coil in frequency domain. Thus, a coil with M turns, having an M x M matrix $\bar{T}$, can exhibit at least M resonances, if not more.

The telegraphist equations (3) and (4) which are valid for TEM waves only, together with the interconnection matrix $\bar{T}$ and boundary constraints, forms the gist of the coupled wave model. As mentioned earlier, however, it represents a first order approximation to the field equations in helical

coordinates. If the coupling coefficients are to be computed analytically from the geometry of the coil, rather than empirically, then a detailed solution of the field equations is necessary.

It would be a mistake to think of the elements of the coupling matrices, L_{mn} and C_{mn}, as distributed inductances and capacitances, because the concept of distributed circuit elements does not always have justification in the electromagnetic field [6]. The important point to keep in mind is that one matrix is porportional to the inverse of the other. Thus when the geometric structure is such that capacitance coefficients can be calculated in the electrostatic sense, e.g., the straight array in Fig. 1 without interconnections, then it is helpful to think of $\overline{C}$ as a capacitance matrix. However, $\overline{L}$ would have no more significance than that of being an inverse. On the other hand, in a coil the $\overline{L}$ matrix is related to the low frequency inductance, as illustrated for a two turn coil in the next section. In this case, the concept of distributed capacitance would be inappropriate, and $\overline{C}$ should be regarded as the inverse of the inductive matrix. In fact, the relation between the inductive coupling matrix of the wave theory and ordinary inductance observed at low frequencies may provide a way for estimating the coupling coefficients.

B. Formal Solution

The system of equations (3) and (4) may be solved formally only to the extent of relating the terminal voltage and current, $v_t(t)$ and $i_t(t)$, to the M voltages and currents on each turn. A complete description of the coil behavior, however, cannot be given without prior specification

of its connections to external components such as generators and damping resistors. As to method of solution, the Laplace transform (over time) offers the most direct route since it also allows inclusion of initial currents. Transforms here are denoted by capital symbols, e.g., $\underline{V}(\zeta,s)$ is the transform of $\underline{v}(\zeta,t)$.

As to be expected, the solution is dominated by properties of the interconnection matrix $\overline{T}$ and the coil geometry as manifested in a characteristic wave admittance matrix defined as

$$\overline{Y}(s) = \eta_o \, \overline{\gamma}(s) \tag{12}$$

where $\eta_o = (\varepsilon/\mu)^{\frac{1}{2}}$ is the wave admittance of the medium surrounding the coil wires. After transformation of the matrix wave equation (6), the general solution is found to be

$$\underline{V}(\zeta,s) = \underline{A}(s)\, e^{-s\zeta/c} + \underline{B}(s)\, e^{s\zeta/c} \tag{13}$$

$$\underline{I}(\zeta,s) = \overline{Y}\,[\underline{A}(s)\, e^{-s\zeta/c} - \underline{B}(s)\, e^{s\zeta/c}] \tag{14}$$

where $\underline{A}$ and $\underline{B}$ are as yet undetermined column vector coefficients. By imposition of the periodic boundary constraints stated in (7) and (8), one determines these vector coefficients in terms of the terminal voltage $V_t(s)$ to be

$$\underline{A}(s) = \sqrt{\beta(s)}\;\; \overline{S}(s)\;\; \overline{P}(s)\, \underline{a}_M\, V_t(s) \tag{15}$$

$$\underline{B}(s) = \sqrt{\beta(-s)}\;\; \overline{S}(-s)\, \overline{P}(-s)\, \underline{a}_M\, V_t(s) \tag{16}$$

where

$$\beta(s) = e^{-s\tau} \tag{17}$$

$$\tau = 2L/c \tag{18}$$

$$\bar{P}^{-1}(s) = \bar{T} - \beta(s)\,\bar{I} \tag{19}$$

$$\bar{S}^{-1}(s) = 2\bar{I} - \bar{G}(s) \tag{20}$$

$$G(s) = \bar{I} - \bar{R}^{-1}(s)\,\bar{Y}^{-1}(s)\,\bar{R}(s)\,\bar{Y}(s) \tag{21}$$

$$\bar{R}^{-1}(s) = \bar{R}(-s) = \beta\bar{I} - (1-\beta^2)\,\bar{P}(s) \quad . \tag{22}$$

It is noticed that the important matrices in this formal solution are the characteristic admittance matrix and the delay matrix $\bar{P}$, defined in (19) in terms of the interconnection matrix $\bar{T}$. Further, the term $\bar{P}\underline{a}_M$ in the expressions for the vector coefficients $\underline{A}$ and $\underline{B}$ is the column vector composed of the M^{th} column of $\bar{P}$. In the particular case of a uniform single layer helix, $\bar{T}$ has the elements defined in (9), so that $\bar{P}$ takes the form

$$\bar{P}(s) = \frac{1}{1-\beta^M}\begin{bmatrix} \beta^{M-1} & \beta^{M-2} & \cdots & \beta & 1 \\ 1 & \beta^{M-1} & \beta^{M-2} & \beta^2 & \beta \\ \beta & 1 & \beta^{M-1} & & \beta^2 \\ \vdots & & & & \vdots \\ & & 1 & & \\ \beta^{M-2} & \beta^{M-3} & \cdots & & \beta^{M-1} \end{bmatrix} . \tag{23}$$

The pattern is such that each row is obtained from the preceeding one above it by shifting and folding the columns one step to the right.

Significantly, this matrix is strictly a function of the delay parameter $\beta = e^{-s\tau}$. Unlike ordinary circuit elements, then, any transfer functions or admittance functions which might characterize the coil as a system would be functions of β rather than the frequency image parameter s.

Translated to time domain, this means that the temporal events within the coil evolve in discrete steps each having a duration $\tau = 2L/c$, which is the time of travel of an electromagnetic disturbance around a single turn. As stated earlier, it is on this time scale that high voltages are likely to occur.

The Laplace transform expressed in terms of the variable $e^{-s\tau}$ instead of the usual s is sometimes called the Z-transform [7], which is found useful in manipulating discrete time sequences. However, so as not to confuse the issue, whereas the Z-transform is applicalbe to time functions that exist only at discrete points and are zero in the intervals between, here the time functions exist during the entire interval making abrupt jumps from one interval to the next. Physically, this behavior is a manifestation of multiple reflections and turn-to-turn coupling. The phenomenon becomes more meaningful in the sample computations on a two-turn coil given in the next section.

We now turn our attention to the terminal admittance which is an important parameter, playing a role in the way the coil interfaces with external components. It is defined as

$$Y_t(s) = \frac{I_t(s)}{V_t(s)} \quad . \tag{24}$$

Since the terminal current, I_t, is the boundary current, $I_1(-L,s)$, of the first turn, the terminal admittance is simply the first row element of the vector solution $\underline{I}(-L,s)$ in Eq. (14). After substitution of (15) and (16) into (14) and using the form of $\bar{P}$, one finds

$$Y_t = \frac{1}{1-\beta^M} \sum_{j=1} \sum_{m=1} Y_{1j} \left[S_{jm}(s)\beta^{m-1} + S_{jm}(-s)\beta^{M-m+1} \right] \quad . \tag{25}$$

It is evident that the problem of calculating Y_t centers around finding the matrix element S_{jm}, which is far from being an easy task. The difficulty arises largely from the fact that two unrelated matrices, $\bar{R}$ and $\bar{Y}$, enter the definition of $\bar{S}^{-1}$ given in (20) and (21). Consequently, some of the well known techniques of analytical inversion, such as expansion in eigenvectors or idempotents, are not readily applicable to any significant advantage. That is, using the eigenvectors of one matrix only complicates the other. A possible technique that might prove useful consists of expanding $\bar{S}$ in an operator power series, suggested by the form of $\bar{S}^{-1}$ given in (20). Thus, assuming that such a series converges, one writes

$$\bar{S} = \tfrac{1}{2} [\bar{I} + \tfrac{1}{2}\bar{G} + \tfrac{1}{4}\bar{G}^2 + \ldots] \quad . \tag{26}$$

Retaining only the first term, $\frac{1}{2}\bar{I}$, we have examined the simplified approximate solution for M turns and found the results to be in accord with the conclusions based on exact analysis of the two-turn coil. It is interesting to note that the first term of $\bar{S}$ yields an exact solution, even in the general case of M turns, under the very special condition when the product $\bar{R}\bar{Y}$ is commutative. For, in that case, as evident from (21), $\bar{G}$ vanishes identically.

At this stage, it appears that a numerical technique utilizing computers offers the only practical course of action. However, because of the magnitude of the task, lying well beyond the scope of this investigation, evolution of computer programs for the general case was not undertaken. Instead, owing to its mathematical tractability, the two-turn coil has been analyzed largely for the purpose of appraising the merit of the model.

C. Two-Turn Coil

Highlights of the reduction of the general solution to the particular case M = 2 are given here to the extent needed for the analysis presented in Sec. III. In this case, the characteristic admittance matrix has only two distinct elements

$$\bar{Y} = \eta_o \begin{bmatrix} \gamma_1 & -\gamma_2 \\ -\gamma_2 & \gamma_1 \end{bmatrix} , \tag{26}$$

while the interconnection matrix takes the simple form

$$\bar{T} = \begin{bmatrix} 0 & 1 \\ 1 & 0 \end{bmatrix} . \tag{27}$$

Under these conditions, the product $\bar{R}\bar{Y}$ is commutative so that the matrix $\bar{S}$ reduces to $\frac{1}{2}\bar{I}$, thus simplifying Eqs. (15) and (16) substantially. The result is

$$\underline{A}(s) = \tfrac{1}{2} V_t(s) \frac{\beta^{\frac{1}{2}}}{1-\beta^2} \begin{bmatrix} 1 \\ \beta \end{bmatrix} \tag{28}$$

$$\underline{B}(s) = -\tfrac{1}{2} V_t(s) \frac{\beta^{\frac{1}{2}}}{1-\beta^2} \begin{bmatrix} \beta \\ 1 \end{bmatrix} \tag{29}$$

Using these coefficients in Eqs. (13) and (14), one can calculate the voltage and current at any point on the two turns. Our interest, however, centers mainly on the terminal admittance function, because this provides a direct way of testing validity of the model. Since $S_{jm} = \delta_{jm}$, Eq. (25) reduces to

$$Y_t(s) = \frac{\eta_o}{2(1-\beta^2)} \left[\gamma_1(1+\beta^2) - 2\gamma_2\beta\right] \quad . \tag{30}$$

Alternately, the admittance may be put in the form

$$Y_t(s) = \frac{\eta_o}{2} \left[\gamma_1 \coth(s\tau) - \gamma_2 \operatorname{csch}(s\tau)\right] \tag{31}$$

which is found more convenient in analysis of steady-state frequency response.

It is evident that even for the two turn-coil, the wave theory admittance Y_t is far from the expression $1/sL_e$ obtained for the lumped inductance L_e found in circuit theory. However, the expression in (31) contains the circuit theoretic form as a limit. This may be shown by expanding the hyperbolic functions in a power series, the first two terms of which are

$$Y_t(s) \rightarrow \frac{\eta_o}{2} \frac{\gamma_1-\gamma_2}{s\tau} \left[1 + \tfrac{1}{2}s^2\tau^2 \frac{\gamma_1}{\gamma_1-\gamma_2}\right] . \tag{32}$$

This asymptotic form would be valid in the low end of the frequency response or, equivalently, in the long term limit of the time domain response. The quantity multiplying the term s^2 in (32) is properly interpreted as a resonance frequency,

$$\omega_o^2 = \frac{2(\gamma_1-\gamma_2)}{\gamma_1\tau^2} \quad . \tag{33}$$

It is also recognized that the asymptotic form of Y_t corresponds exactly to the admittance of a hypothetical circuit comprised of an inductor and capacitor in parallel having values

$$L_e = \frac{2\tau}{\eta_o(\gamma_1 - \gamma_2)} \tag{34}$$

$$C_e = \frac{\gamma_1 \eta_o \tau}{4} \tag{35}$$

While L_e can be related to the quasistatic inductance of a coil as given by the Neumann formula [8], one would be hard pressed to find field theoretic justification for a coil capacitance having the above value C_e. This point emphasizes the limitations of the circuit theoretic approach. That the inductance coupling matrix elements are related to the quasistatic inductance is a consequence of our assumption that the waves on a coil behave as transverse electromagnetic (TEM) waves [9].

III. TESTS ON A TWO-TURN COIL

A. Frequency Response

The frequency response of a coil, as seen at its terminals, is essentially a manifestation of its terminal admittance function. In a typical experiment, one observes the terminal current as a function of frequency. It is best, therefore, to examine this current when the coil is connected to an oscillator whose voltage and output resistance are $V_g(j\omega)$ and R_g, respectively, where ω is the angular frequency and $j = \sqrt{-1}$. The terminal current phasor is then

$$I_t(j\omega) = V_g(j\omega) \frac{Y_t(j\omega)}{1 + R_g Y_t(j\omega)} \quad . \tag{36}$$

To convert $Y_t(s)$ from (31) to phasor form, one simply makes the substitution $s = j\omega$ to obtain

$$I_t(j\omega) = R_g^{-1} V_g(j\omega) \frac{y_1 \cos(\omega\tau) - y_2}{y_1 \cos(\omega\tau) - y_2 + j \sin(\omega\tau)} \tag{37}$$

where

$$y_i = \tfrac{1}{2}\eta_o \gamma_i R_g, \quad i = 1,2 \tag{38}$$

are the normalized admittance matrix elements.

Inspection of (37) reveals that, for values $y_1 \neq 0$ and $y_2 \neq 0$, the magnitude of the current reaches a maximum when the imaginary term in the denominator vanishes, and a minimum when the numerator vanishes. That is, for integer values of m and n, the maxima occur at uniformly spaced frequencies,

$$\omega_m = m\pi/\tau \quad , \tag{39}$$

and the minima at non-uniformly spaced frequencies,

$$\omega_n = \frac{1}{\tau}\left[\cos^{-1}(\gamma_2/\gamma_1) + 2n\pi\right] \quad . \tag{40}$$

It is evident that the turn-to-turn coupling plays a significant role in determining the minima of the frequency response. Typical graphs of normalized current vs. $\omega\tau$ are shown in Fig. 3 for two values of the ratio y_2/y_1. In the absence of coupling, $y_2 = 0$, the minima become uniformly spaced at odd multiples of $\pi/2$. This is the result one would obtain if the entire length of both turns of the coil were treated as a single uncoupled transmission line, as was done in the earlier work [2]. However, in the presence of coupling, the maxima are not affected, but the minima are shifted symmetrically toward the even numbered maxima. The lowest minimum, lying near $n = 0$, is interpreted as the low frequency resonance commonly observed in all coils. As it is apparent from (40), when $\gamma_2 = \gamma_1$ implying perfect coupling, the lowest resonance frequency approaches zero. Interestingly, this resonance is actually repeated periodically at higher frequencies. Thus, even the low frequency resonance, which heretofore has been interpreted in terms of distributed capacitance, is seen to be a manifestation of coupled waves. Finally, recalling that $\tau = 2L/c$ where $2L$ is the length of one turn, one observes that the relationship between wire length and resonance frequency in (40) is not simple enough that it could be readily inferred from experimental data. Certainly, in a coil with a larger number of turns the relationship is expected to be more involved. This explains why in our earlier work [2], no simple relationship between wire length and the low resonance frequency was discernible in the data.

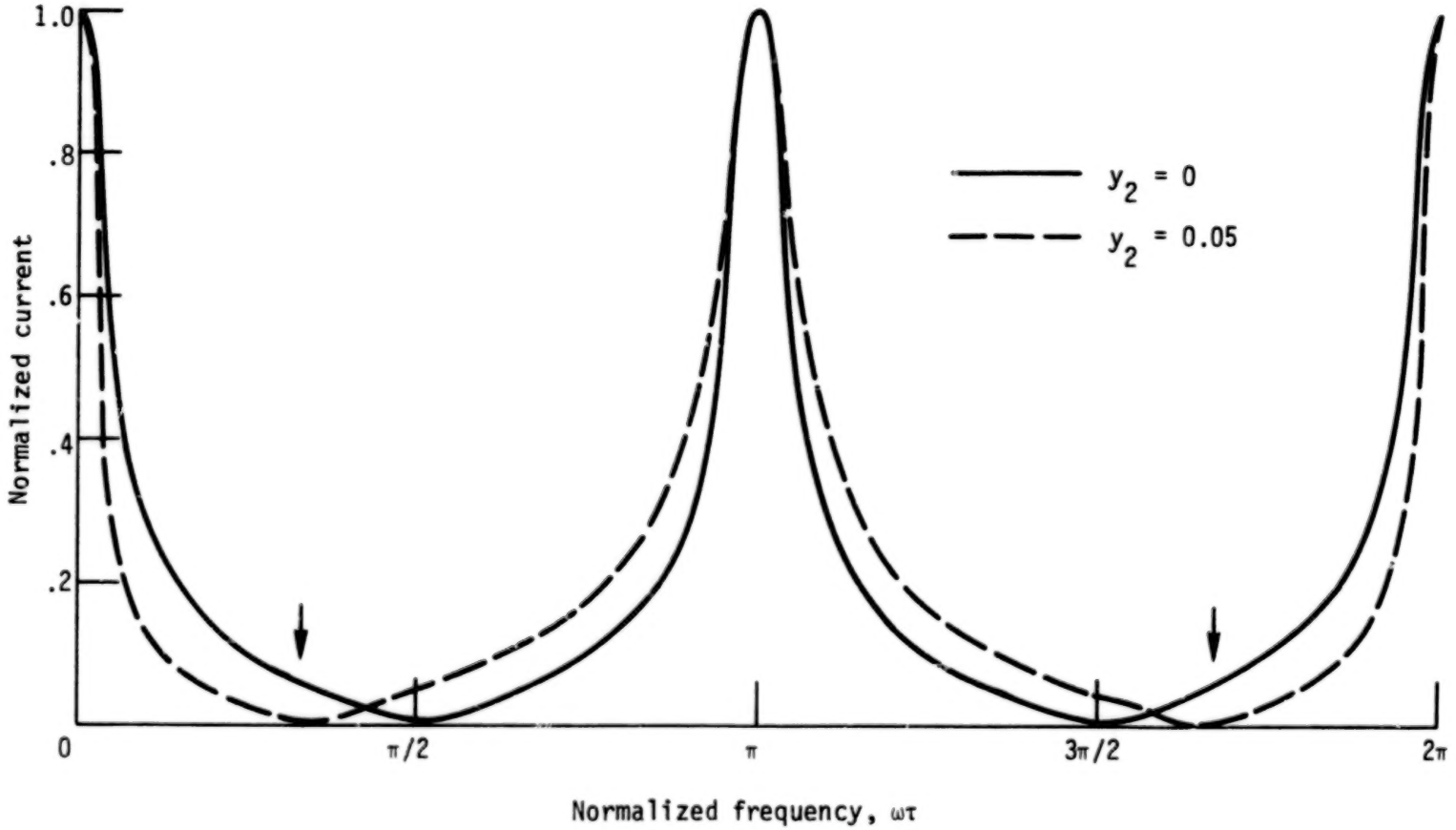

Fig. 3: Typical frequency responses, y_1 = 0.1.

B. Decay of Initial Current

One of the questions which is of central importance to this investigation concerns response of the coil when its terminals are suddenly switched from a power source to a damping resistor R_g. We consider this now for a two-turn coil. Prior to switching, the current within the coil is assumed to have reached a steady state value of I_o which is uniformly distributed. In that case, the voltages anywhere on the coil would necessarily be zero. Conditions immediately after switching, however, are not so obvious.

In this context, two points are worth noting. First, if the coil were viewed as the lumped inductor of circuit theory, the terminal voltage immediately after switching would jump abruptly to a value $-I_o R_g$, and at no time thereafter would the voltage anywhere within the coil exceed this value. In the field theoretic viewpoint, however, placement of a resistor has the significance of a boundary constraint relating only the terminal voltage to the terminal current, and the latter need not necessarily be I_o at the instant of switching.

The second point concerns the meaning of R_g as the apparent resistance experienced by the coil at its terminals. Thus, if the physical resistor is coupled to the coil via any length of wire or cable, then the pertinent value R_g is that obtained by impedance transformation appropriate to transmission lines. Indeed, the effective impedance referred to the coil terminals might not even be purely resistive unless the cable impedance is matched to the resistor. We assume this to be the case.

When an initial current I_o is included, the system of equations (3) and (4) leads to the general solution

$$\underline{V}(\zeta,s) = \underline{A}(s)\, e^{-\zeta s/c} + \underline{B}(s)\, e^{\zeta s/c} \tag{41}$$

$$\underline{I}(\zeta,s) = \overline{Y}\, [\underline{A}(s)\, e^{-\zeta s/c} - \underline{B}(s)\, e^{\zeta s/c}] + \frac{1}{s} I_o \tag{42}$$

where the coefficients $\underline{A}$ and $\underline{B}$ have the same expressions (15) and (16) as the initially uncharged case. Since the terminal current $I_t(s)$ is the boundary current $I_1(-L,s)$, the following conditions must prevail

$$V_t(s) = -I_1(-L,s) R_g \tag{43}$$

$$I_1(-L,s) = V_t(s)\, Y_t(s) + \frac{1}{s} I_o \quad . \tag{44}$$

Equation (43) is merely the condition imposed by the resistor, while (41) follows from (42) and the definition of $Y_t(s)$ given in (24). Combining these two conditions yields the desired terminal current

$$I_t(s) = \frac{1}{s}\, I_o\, \frac{1}{1 + R_g\, Y_t(s)} \quad . \tag{45}$$

From this expression, which is valid for any number of turns, one concludes that the response of the coil under the above conditions is equivalent to excitation of an initially uncharged coil by a step voltage $-I_o R_g$ through a series resistor R_g. This is also true of any transmission line.

It is convenient to deal with a normalized terminal current I_t' defined as I_t/I_o. After substituting (30) into (45) one obtains for the two-turn coil,

$$I_t'(s) = \frac{1}{s}\, \frac{1 - \beta^2}{(1+y_1) - 2y_2\beta - (1-y_1)\beta^2} \tag{46}$$

where y_1 and y_2 are defined in (38). Inasmuch as the denominator is a polynomial in $\beta = e^{-s\tau}$ instead of s, the inverse of (46) consists of discrete steps in intervals of duration τ. This is manifested effectively by expansion of (46) in a power series in β, as outlined in the Appendix. The procedure also facilitates numerical evaluation of the inverse, $i_t'(t)$, by means of a digital computer. The result is the sequence of steps

$$i_t'(t) = \sum_{n=o}^{\infty} K_n' \, u(t - n\tau) \tag{47}$$

where u(t) is the unit step function and K_n' are determined from the roots of the quadratic in the denominator of (46).

Note that the sum in (47) is cumulative, so that the value of i_t' at the N^{th} transition is the sum of the first N coefficients. That is,

$$i_t'(t) = S_N = \sum_{n=o}^{N} K_n', \quad N\tau < t < (N+1)\tau \quad . \tag{48}$$

Since the time is indexed in discrete intervals, the sequence S_N which is a function of the integer N, is also essentially a function of time. Thus, whether i_t' decreases or increases monotonically, or whether it oscillates in time depends on the behavior of the sequence S_N as a function of N. This in turn is determined by the quantity

$$b = [1 - y_1^2 + y_2^2]^{\frac{1}{2}} \quad . \tag{49}$$

When $b^2 > 0$, the sequence decreases monotonically after the first few steps following t = 0. When $b^2 < 0$, the sequence breaks into oscillation whose period is determined by the values of y_1 and y_2 as well as their ratio y_2/y_1. This condition is reminsecent of the underdamped and

overdamped RLC circuit. Indeed, if one were to observe the current decay on instruments having insufficient bandwidth, the sequence would appear as a smoothed curve much as the response of an ordinary circuit.

The above features are illustrated in a selection of graphs shown Figs. 4 through 8 , which were obtained by the use of a digital computer. Two of these figures are worth singling out. In Fig.6 during the second interval the current jumps to 1.125 times the value of the initial current, unlike the circuit theoretic behavior. Similarly, the voltage is 1.125 times $I_o R_g$. This excess occurs when y_2/y_1 approaches unity (perfect coupling) and y_1 is 0.33, the latter being a condition that depends on the choice of R_g. Effects of compression of time scale are shown in Fig. 8 for the underdamped case, $b^2 < 0$. In particular, the period of oscillation here, as one might expect, is related to the low frequency resonance discussed in the previous section. If we define $N_p\tau$ to be this period, then it can be shown that the frequency is

$$\frac{2\pi}{N_p\tau} = \frac{1}{\tau} \tan^{-1} \left[\frac{(y_1^2 - y_2^2 - 1)^{\frac{1}{2}}}{y_2}\right] \tag{50}$$

which is related to the low resonance frequency via (40) with n = 0. It is important to note that this oscillation can be easily suppressed by the simple expediency of proper choice of R_g. However, this would not eliminate the possibility of high voltage buildup because this occurs in the overdamped case as seen in Fig. 6 . This theoretical conclusion which is based on the simple configuration of two-turns agrees with the earlier experiments on a multiturn coil [2] where the

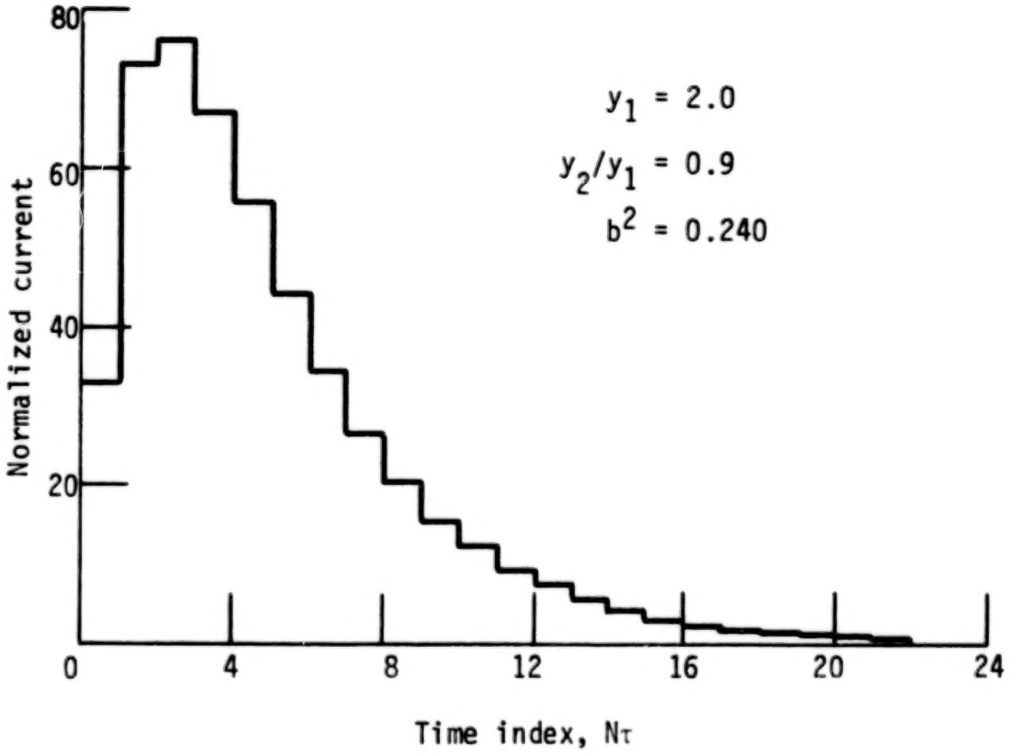

Fig. 4: Decay of initial current in short time scale, over-damped. I_o = 100.

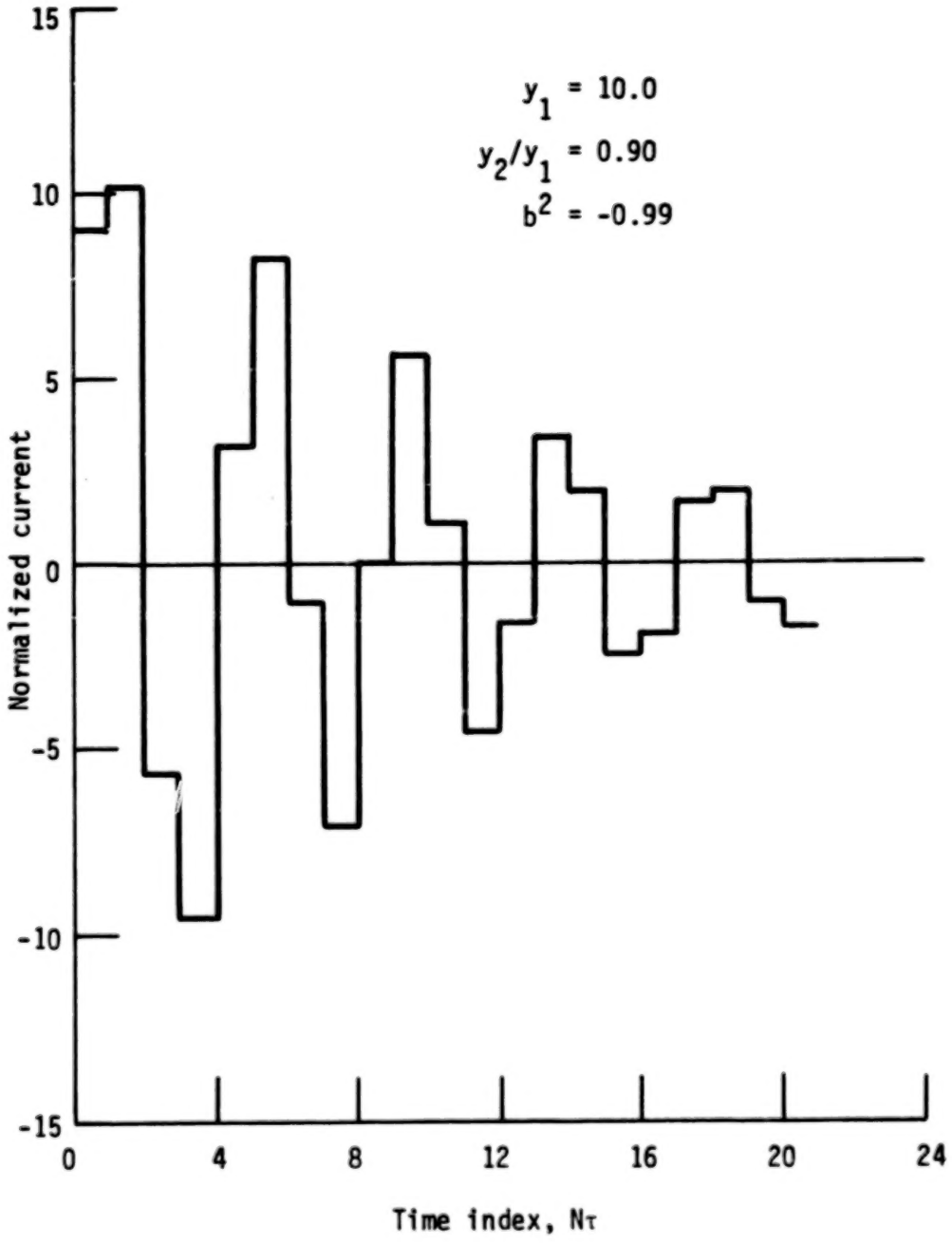

Fig. 5: Decay of initial current in short time scale, underdamped case. $I_o = 100$, $N_p = 4$.

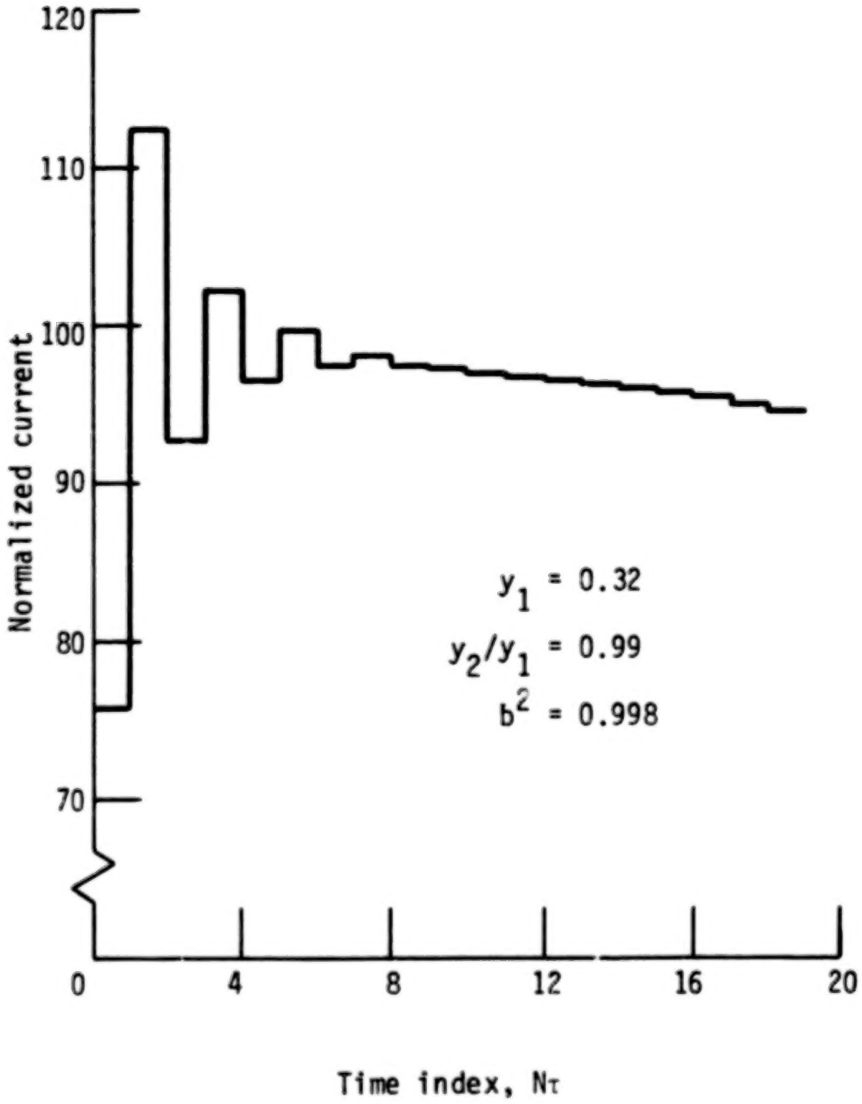

Fig. 6: First few steps of current decay under conditions when it exceeds I_o = 100.

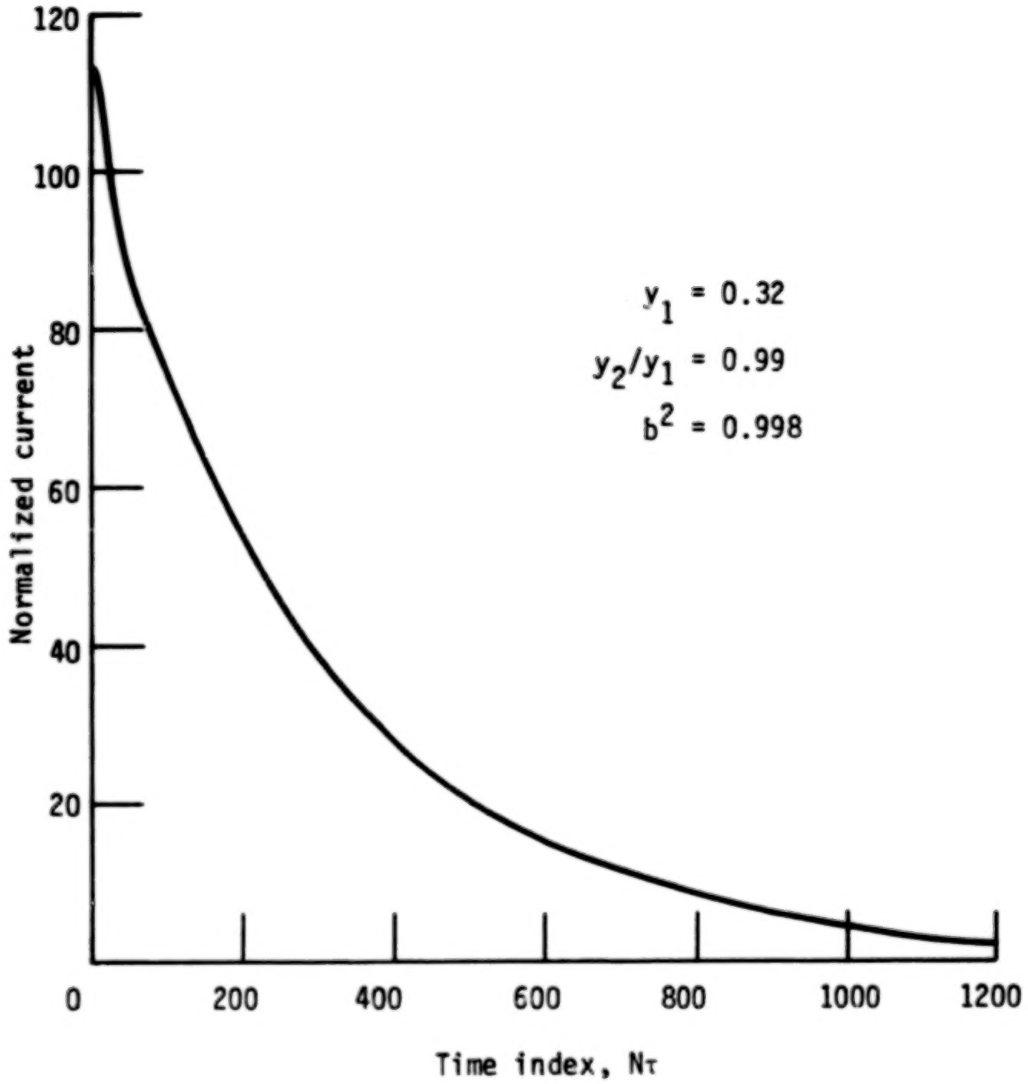

Fig. 7: Decay current of Fig. 6 on compressed time scale.

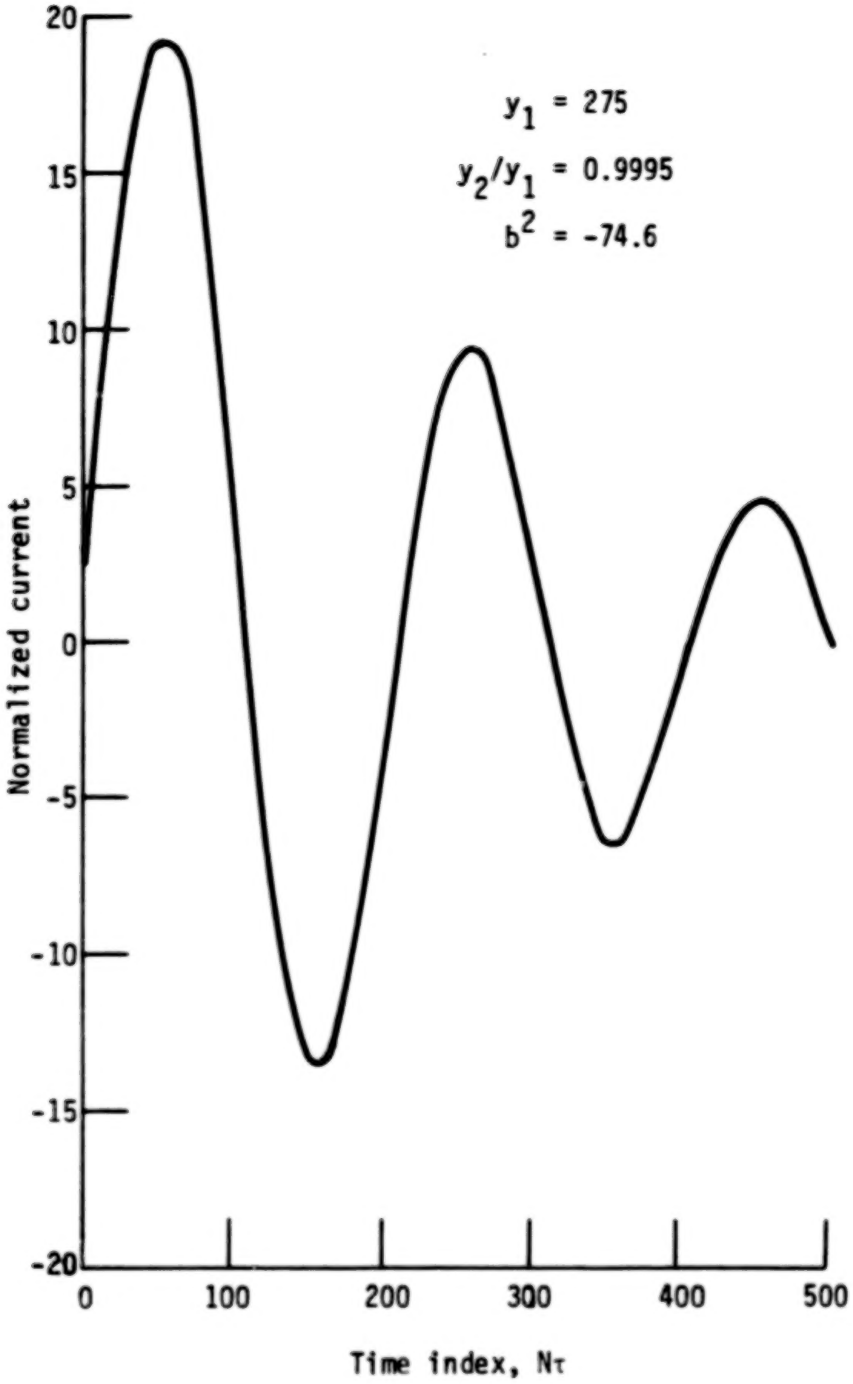

Fig. 8: Decay of initial current in underdamped case on compressed time scale. I_o = 100; N_p = 201.

low frequency ringing was successfully suppressed by choice of resistor, which had otherwise little effect on multiple step reflections.

Returning to the overdamped case, one observes by inspection of (46) that because of the numerator the current is actually the difference between a sequence and its delayed replica, displaced by the interval 2τ. The denominator shows that this sequence increases monotonically, reaching the limiting value $1/2(y_1-y_2)$ as obtained by setting $s = 0$. As evident, this limiting value grows without bounds as y_2 approaches y_1 with increasing coupling. However, because one sequence is delayed by an exact multiple of the uniform duration of each step, the subtraction is complete resulting in a decreasing net response. It is conceivable that when the durations of the steps in the sequences are not the same, a high voltage pulse might occur due to incomplete cancellation. This situation is possible in a multilayer solenoid, for example, where travel times per turn differ from layer to layer. By this line of reasoning, one tentatively concludes that dielectric breakdown between adjacent layers is more likely than between turns of the same layer.

C. An Experimental Test

Time domain reflectometry (TDR) offers a simple and direct means for an experimental appraisal of the model. In a pulsed TDR experiment, one measures not only reflection coefficients but also pulse travel times. Typically, a cable with known characteristics is connected to a pulse generator on one end and to the test component on the other, as shown in Fig. 9 . The signal reflected from the termination, which is displayed on an oscilloscope coupled to the generator end, is determined by the

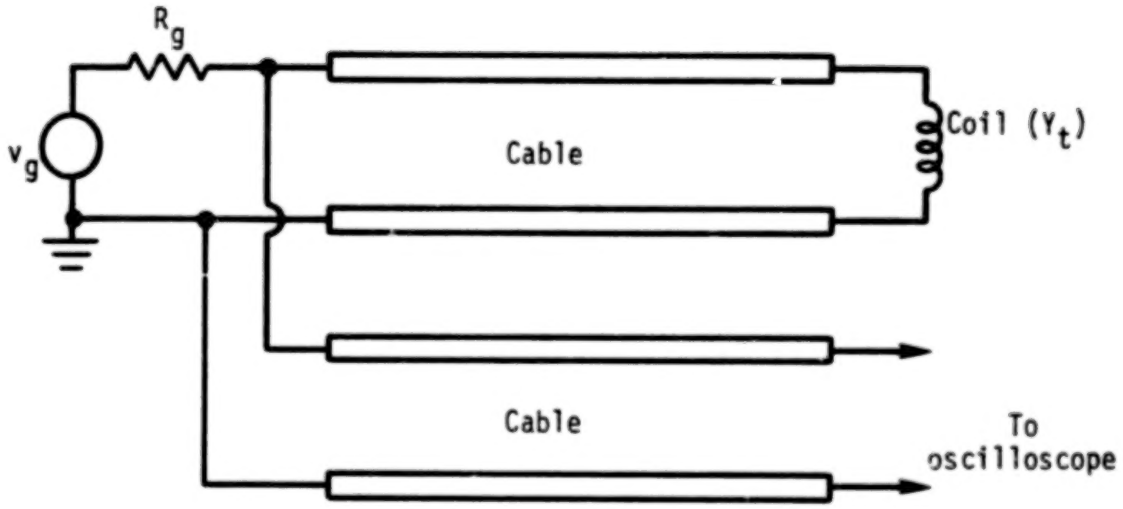

Fig. 9: Schematic diagram for pulse TDR experiments.

reflection coefficient defined in terms of the cable admittance Y_o and the terminal admittance $Y_t(s)$ as

$$\rho_t(s) = \frac{Y_o - Y_t}{Y_o + Y_t} \quad . \tag{51}$$

It is well known in the theory of transmission lines that if the generator is matched to the cable and its voltage is $V_g(s)$, then the observed reflected voltage $V_r(s)$ at the generator terminal is given by

$$V_r(s) = V_g(s)\ \rho_t(s)\ e^{-s\tau_o} \tag{52}$$

where τ_o is the fixed delay due to the cable length, which is not of consequence. Except for this fixed delay, the reflected signal $v_r(t)$ in time is essentially the convolution of $v_g(t)$ and the inverse of $\rho_t(s)$. After substitution of $Y_t(s)$ given in (30) into (51), the inversion may be effected most conveniently by expanding the result in powers of $\beta = e^{-s\tau}$. The reflected signal once again is found to be an infinite sequence of successively delayed terms of the form

$$v_r(t) = \sum_{n=0}^{\infty} \rho_n\ v_g(t - n\tau) \tag{53}$$

where the time origin has been shifted to suppress the fixed delay τ_o. Thus, if the duration of the generator pulse form $v_g(t)$ is shorter than the coil travel time τ, each term in the sequence is distinctly resolved. However, owing to the damping arising from the finite resistivity of the coil wire at room temperature, only the first few terms are observable experimentally.

According to the theory, the first term, ρ_o, is due to the discontinuity at the coil terminals and depends only on the diagonal element γ_1. The second term, ρ_1 arriving τ units later, is proportional to the mutual coupling element γ_2; while the third term, ρ_3, arriving 2τ units later is dependent on γ_1 and γ_2, and so on. The arrival times are very significant. For, when γ_2 vanishes in the absence of mutual coupling, the theory shows that the successively reflected terms would be separated by intervals of 2τ units corresponding to travel around the entire length of the two turns. The fact that, theoretically, the reflected pulses are separated by intervals corresponding to travel around one turn and the fact that the second term is proportional to the mutual coupling are two important data amenable to experimental verification.

Typical experimental reflection patterns are shown in Figs. 10 and 11 for loose coupling and tight coupling. The coil under test consists of two turns of No. 22 enameled copper wire wound on a wooden form having a diameter of 2.0 ft. In the tightly coupled coil, the wires are separated essentially by the enamel thickness, while in the loosely coupled case they are separated by 1/8 inch nominally. The travel time, τ, should be roughly 8.2 nsec as determined from measurement of the propagation speed on a pair of straight sections of the same wire laid out as a transmission line. This measurement yielded 1.3 nsec per ft.

As evident from Figs. 10 and 11, the timing of the pulses and the variation of the second pulse amplitude with coupling are in qualitative

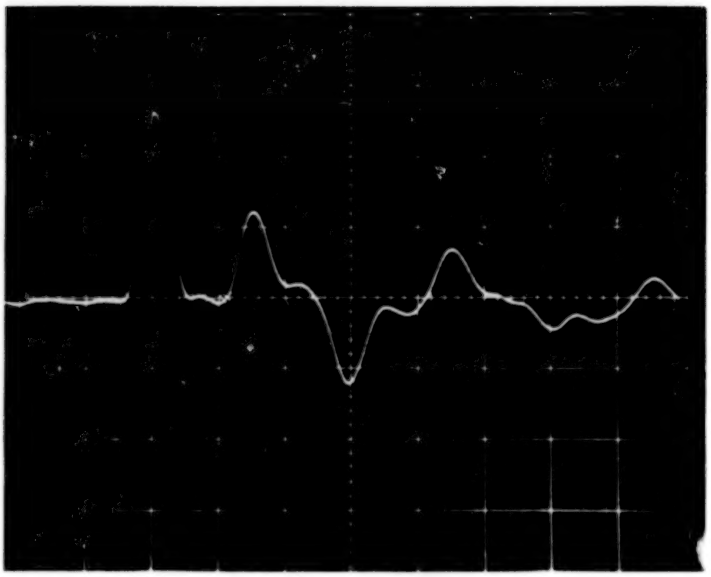

Fig. 10: Pulse reflection pattern from a loosely coupled two-turn coil. Scale: 5 nsec/cm

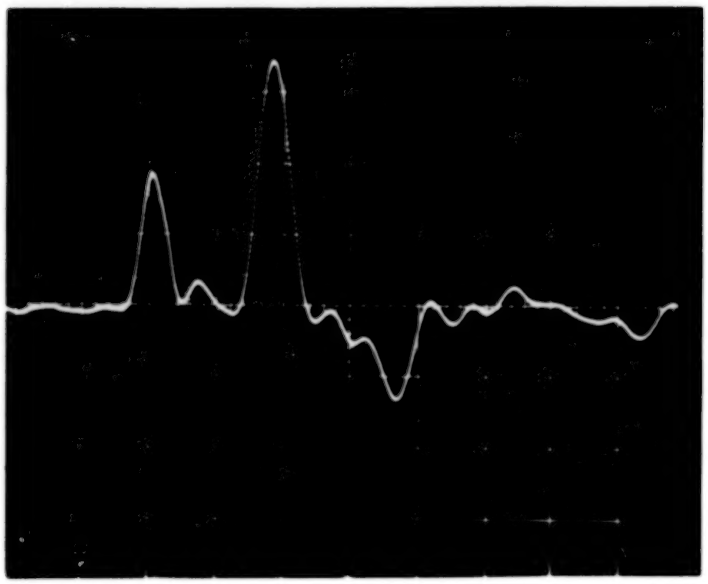

Fig. 11: Pulse reflection pattern from a tightly coupled two-turn coil. Scale: 5 nsec/cm

agreement with the theory. In the absence of an analytical relationship between the coupling coefficients and coil geometry, however, quantitative comparisons cannot be made at this stage of development. It is noticed, also, that in the tightly coupled case the travel time increases slightly. This effect is attributed to the finite resistivity of the wire which is not included in the model equations for simplicity. However, when it is introduced as an additive diagonal matrix, the product of the inductive and capacitive matrices would no longer be $1/c^2$, but it would depend on the relative magnitudes of resistivity and coupling coefficients.

The physical mechanism underlying the observed patterns may be visualized with the aid of Fig. 12. To do so, one must keep in mind that the observable voltages are ultimately representations of the charge distribution on the wires. When such voltages are transmitted along a uniform cable they are associated with a positive charge distribution on one conductor and a negative (image) charge distribution on the other, both traveling in unison. Thus, an incident positive voltage pulse arriving at the coil means that terminal 1 receives a positive charge pulse, while terminal 2 receives an equal negative charge pulse. Due to the discontinuity, however, a fraction of these pulses is returned to the generator end, appearing as the first reflected term. The mismatch between the cable and coil terminals determines the polarity of the first reflected term relative to that of the incident one. We consider here the positive case.

Now suppose that there is no coupling between turns. Then the pulses entering the terminals travel independently, but in opposite direction, down the entire length of the coil, the positive pulse arriving at terminal 2 and the negative pulse at terminal 1. As evident, the

fractions of these pulses entering the cable and returning to the generator end have polarities opposite to those of the incident pulses and their arrival time is 2τ units later than the first reflected pulse. All successively reflected pulses would be separated by the interval 2τ.

On the other hand, if there is coupling, each of the incident pulses, a and b in Fig. 12, induces a pulse of opposite polarity in the neighboring turn. These secondary pulses, c and d, travel in unison with their respective primary pulses, but they arrive at the terminals after traversing only one turn corresponding to a delay of τ units relative to the first reflected pulse. Moreover, they enter the cable and return to the generator end in the same polarity as the incident pulse. Thus, turn-to-turn coupling causes a periodicity in the coil response, having intervals related to one turn. Another periodic interval results from the overall length of the coil.

Extending this line of reasoning to a multilayer solenoid, one concludes that a coil should manifest periodicities related to the wire length between any neighboring points that are tightly coupled. A layer-wound solenoid having M turns per layer may be viewed as a single coil that is folded on itself at intervals of M turns. The first turn in the first layer is then coupled to the $2M^{th}$ turn which lies in the next layer. Consequently, the coil response should also manifest periodicities at intervals $2M\tau$, i.e., intervals determined by the spiral length of a layer. Such layer related periodicity has been observed [2].

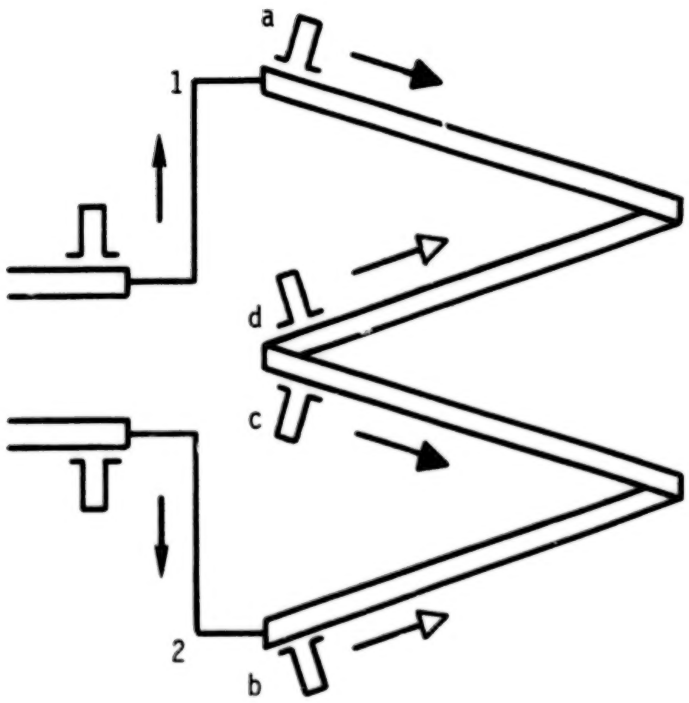

Fig. 12: Schematic illustration of pulse travel around two-turn coil.

IV. CONCLUSION AND RECOMMENDATIONS

We have evolved basically the skeletal structure of an analytical model for coils which, unlike earlier models, is founded on principles of electromagnetic field theory. Despite the fact that it incorporates only the essential features of coupled wave phenomena, the model is remarkable in its agreement with several facts observed experimentally. The single most important finding demonstrated on a two turn coil is the discrete nature of time domain responses which unfold in steps having the characteristic duration related to a single turn of winding. This feature alone is sufficient to indicate the inadequacy of circuit theoretic modeling. Where high voltages are concerned, the analysis of a two-turn coil has illustrated that through the mechanism of wave reflection the terminal voltage can exceed that predicted by circuit theory. In this highly simplified configuration, having only two degrees of freedom, the coil terminals are the only location where an excessive voltage materializes. Given the larger number of degrees in multiturn coils, it is conceivable that high voltages could develop at several locations within the coil. As discussed in Sec. III.B, any inhomogeneity in travel times per turn, owing to variations in the radii of layers or turns, appears to be a likely predisposing condition for high voltages to occur.

The pertinent parameters have been identified to be the wave coupling coefficients as manifested in the admittance matrix $\overline{Y}$ and the characteristic travel time of a wave front around a single turn. At this stage, however, any firm conclusions on design criteria would be premature and ill-founded. Such criteria cannot be conclusively defined without

further exhaustive analysis which might proceed in two phases. The first would consist of a detailed exploration of the general matrix solutions given in Sec. II.B, based on a hypothetical selection of parameters to determine their causative relation to the overall electrodynamic behavior of multiturn coils. The second would be directed at determining the relationship between physical features of the coil and those parameters which have been found theoretically to be most pertinent. Only after such conclusive analysis can any meaningful specifications be cited for such physical features as wire size, wire cross sectional shape, and packing factor, all of which have direct bearing on the magnitudes of coupling coefficients. It is not difficult to estimate intuitively and from experience the way the coupling coefficients might vary with the above features. However, the significant but inconclusive aspect is the link between these coefficients and the coil behavior when large numbers of turns are involved.

Success of the computational and experimental tests on the two-turn coil indicates that the coupled wave model has sufficient merit to warrant further evolution and refinement. Among the desirable features which should be included in the future are effects of: line-of-sight radiative coupling, finite resistivity of windings, and inhomogeneities in travel times. While the resistivity and travel time are of primary concern, the radiative coupling is not, save for the fact that it might account for the fine structure parasitic oscillations generally observed on TDR traces for all coils examined in this investigation.

Finally, no investigation of high speed electromagnetic transients on superconducting coils would be realistic without serious attention

directed to questions concerning the current distribution over the wire cross section. Given the typical configuration of copper clad superconductor fibers, it is quite certain from the Maxwell field theory that the current associated with any externally initiated disturbance would reside at the surface of the copper substrate. The more difficult question, however, concerns the way a large current initially confined within the superconducting fibers might distribute itself when it is suddenly subjected to a disturbance in the neighborhood of the associated high magnetic field. Whatever the origin of superconductivity on the atomic scale, its macroscopic manifestation is an enormously large conductivity, of the order of 10^{25} mho/m. Even the smallest practical fiber is large enough that the Maxwell theory would be very much in command of events. The theory of skin effect indicates that, given the high conductivity, a disturbance occuring at a rate as slow as one cycle per second is sufficient to force the current to the surface of the superconductor. Such disturbances could result, for example, from slow movements of the coil winding under magnetic stresses. Although the distribution of dynamic currents in a superconductor is not fully understood, the skin effect in normal conductors suggests that the fiber currents could leak into the surrounding copper substrate, thus introducing local heating and possibly a quench. Considerations of thermal stability notwithstanding, it would appear that spreading the superconductor as a thin film on the outer periphery of the copper wire would be preferable from the standpoint of electrodynamic stability. This is merely a hypothetical remedy, but clearly questions pertaining to the current distribution deserve careful research as an inseparable part of the overall problem of coil protection.

APPENDIX
INVERSION OF TRANSFORMS

Laplace transforms of functions encountered in analysis of multiply reflected waves typically have the form

$$F(s) = \frac{H(s)}{Q(\beta)} \quad , \qquad \beta = e^{-s\tau} \tag{A.1}$$

where $Q(\beta)$ is a polynomial in β. Such transforms may be inverted by the standard contour integration in the complex s-plane resulting invariably in an infinite sum of residues on account of the periodicity of $e^{-s\tau}$. A more useful sum for our purposes, however, is obtained by first expanding $1/Q(\beta)$ in partial fractions followed by expansion in a power series in β. This method is convenient for digital computations and it elucidates the delay feature inherent in multiple reflections. Thus, in the particular case when $Q(\beta)$ is a quadratic having roots β_1 and β_2, one obtains

$$F(s) = \frac{H(s)}{\beta_2-\beta_1} \left[\frac{1}{\beta_1-\beta} - \frac{1}{\beta_2-\beta} \right] . \tag{A.2}$$

In regions of the s-plane where $|\beta| < |\beta_1|$ and $|\beta_2|$, each of the fractions may be expanded as a geometric series,

$$F(s) = \frac{H(s)}{\beta_2-\beta_1} \sum_{n=0}^{\infty} (\beta_2^{-n-1} - \beta_1^{-n-1})\, e^{-ns\tau} \quad . \tag{A.3}$$

One sees readily that, by the shifting property of the Laplace transformation, the inverse f(t) is the sum of a sequence of delayed and weighted values of h(t)

$$f(t) = \sum_{n=0}^{\infty} K_n\, h(t-n\tau), \tag{A.4}$$

where K_n represents the coefficients in (A.3). Although this sum is similar to Z-transforms in appearance, it differs in one respect, namely, h is defined throughout the entire interval $n\tau$ to $(n+1)\tau$.

In the particular case of the decay of initial current, Sec.III.B, H(s) has the form

$$H(s) = \frac{I_o}{s}(1-\beta^2).$$

Consequently, the inverse is the difference of two sequences

$$i_t'(t) = \sum_{n=0}^{\infty} K_n[u(t-n\tau) - u(t-n\tau-2\tau)] \quad . \tag{A.5}$$

When the index in the second term is shifted, one obtains a single sum

$$i_t'(t) = \frac{1}{1+y_1}\, u(t) + \sum_{n=1}^{\infty} [K_{n+1} - K_{n-1}]\, u(t-n\tau) \tag{A.6}$$

where for the two turn coil,

$$K_n = (1+y_1)^{-n} \quad [(y_2+b)^n - (y_2-b)^n]$$

and b is defined in (49). In the underdamped case, when $b^2 < 0$, one can conveniently group the terms as trigonometric functions thus manifesting oscillation. Omitting details here in the interest of brevity, we indicate that with b = ja, the typical n^{th} term q_n in the sum (A.6) takes the form

$$q_n = c_n \sin[n\theta - \phi]$$

where

$$\tan\theta = a/y_2; \quad \tan\phi = y_1 \tan\theta.$$

Since the index n is essentially the time, it is seen that θ basically defines the frequency of oscillation as given in (50).

REFERENCES

1. Maddock, B J. and James, G. B., Proc. IEEE, vol. 115, p. 543, 1968.

2. Gabriel, G. J. and Burkhart, J. A., Proc. 7th Symp. Engineering Problems in Fusion Research, vol. I, p. 741, 1977 (IEEE Pub. no. 77CH1267-4-NPS) Also Technical Memorandum, NASA TM-73808.

3. Fergestad, P. I. and Henricksen, T., IEEE Trans. PAS, vol. 93. p. 510, 1973.

4. McNutt, W. J., Blalock, T. J., Hinton, R. A., IEE Trans. PAS, vol. 93, p. 457, 1973.

5. McWhirter, J. H., Fahrnkopf, C. D., and Steele, J. H., AIEE Trans. PAS, vol. 75, p. 1267, 1956.

6. Gabriel, G. J., Proc. IEEE, vol. 68, March 1980.

7. McGillem, C. D. and Cooper, G. R., Continuous and Discrete Signal and System Analysis, New York, Holt Rienhart and Wilson, 1974.

8. Silvester, P., Modern Electromagnetic Fields, Englewood Cliffs, N.J., Prentice-Hall, p. 161, 1968.

9. Gabriel, G. J., Proc. IEEE, (to be published).

1 Report No. NASA CR-3332	2 Government Accession No.	3 Recipient's Catalog No.
4 Title and Subtitle COUPLED WAVE MODEL FOR LARGE MAGNET COILS		5 Report Date September 1980 6 Performing Organization Code
7 Author(s) G. J. Gabriel		8 Performing Organization Report No. E-535 10 Work Unit No.
9 Performing Organization Name and Address University of Notre Dame Notre Dame, Indiana		11 Contract or Grant No. NSG-3182 13 Type of Report and Period Covered Contractor Report
12 Sponsoring Agency Name and Address National Aeronautics and Space Administration Washington, D.C. 20546		14 Sponsoring Agency Code

15 Supplementary Notes

Final report. Project Manager, James A. Burkhart, Wind and Stationary Power Division, NASA Lewis Research Center, Cleveland, Ohio 44135.

16 Abstract

A wave coupled model based on field theory is evolved for analysis of fast electromagnetic transients on superconducting coils. It is expected to play a useful role in the design of protection methods against damage due to high voltages or any adverse effects that might arise from unintentional transients. The significant parameters of the coil are identified to be the turn-to-turn wave coupling coefficients and the travel time of an electromagnetic disturbance around a single turn. Unlike the circuit theoretic inductor, the coil response evolves in discrete steps having durations equal to this travel time. It is during such intervals that high voltages are likely to occur. The model also bridges the gap between the low and high ends of the frequency spectrum.

17 Key Words (Suggested by Author(s)) Superconducting magnet coil; Electron[illegible] transients; Coil protection; High volt[illegible] breakdown; Coupled wave theory	18 Distribution Statement Unclassified - unlimited STAR Category 31		
19 Security Classif. (of this report) Unclassified	20 Security Classif. (of this page) Unclassified	21 No. of Pages 52	22 Price* A04

* For sale by the National Technical Information Service, Springfield, Virginia 22161

NASA-Langley, 1980

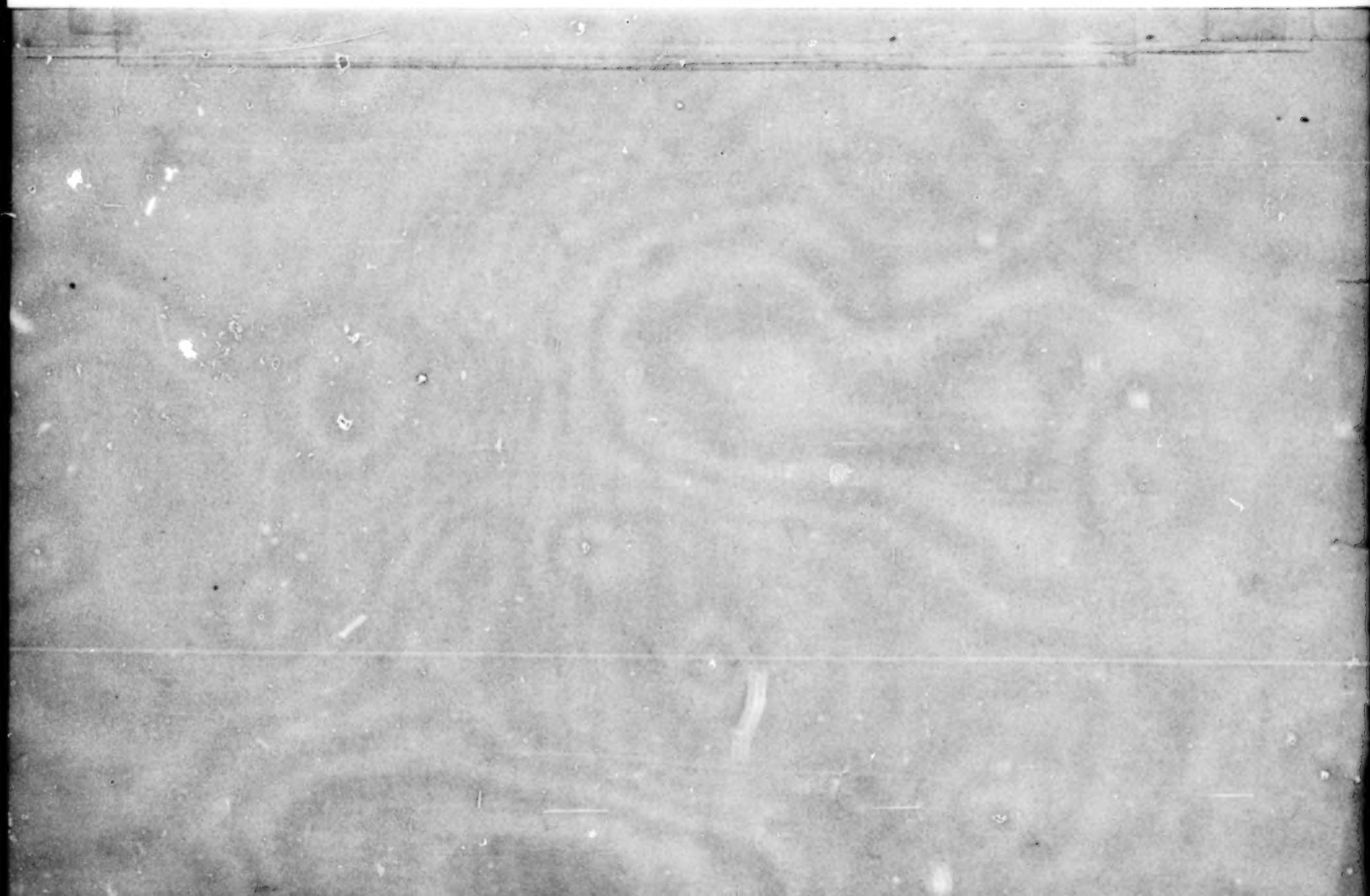

END

December 4, 1980